Human Molecular Genetics, 2014, Vol. 23, No. 5 **1320–1332**
doi:10.1093/hmg/ddt522
Advance Access published on October 22, 2013

Exome sequencing and functional analyses suggest that *SIX6* is a gene involved in an altered proliferation–differentiation balance early in life and optic nerve degeneration at old age

Adriana I. Iglesias[1], Henriët Springelkamp[1,2], Herma van der Linde[3], Lies-Anne Severijnen[3], Najaf Amin[1], Ben Oostra[1], Christel E. M. Kockx[4], Mirjam C. G. N. van den Hout[4], Wilfred F. J. van IJcken[4], Albert Hofman[1], André G. Uitterlinden[1,5], Rob M. Verdijk[6], Caroline C. W. Klaver[1,2], Rob Willemsen[3,†] and Cornelia M. van Duijn[1,†,*]

[1]Department of Epidemiology, [2]Department of Ophthalmology, [3]Department of Clinical Genetics, [4]Center for Biomics, Department of Cell Biology, [5]Department of Internal Medicine and [6]Department of Pathology, Erasmus University Medical Center, Rotterdam, The Netherlands

Received August 6, 2013; Revised and Accepted October 17, 2013

Primary open-angle glaucoma (POAG) is a hereditary neurodegenerative disease, characterized by optic nerve changes including increased excavation, notching and optic disc hemorrhages. The excavation can be described by the vertical cup–disc ratio (VCDR). Previously, genome-wide significant evidence for the association of rs10483727 in *SIX1–SIX6* locus with VCDR and subsequent POAG was found. Using 1000 genomes-based imputation of four independent population-based cohorts in the Netherlands, we identified a missense variant rs33912345 (His141Asn) in *SIX6* associated with VCDR ($P_{meta} = 7.74 \times 10^{-7}$, $n = 11\,473$) and POAG ($P_{meta} = 6.09 \times 10^{-3}$, $n = 292$). Exome sequencing analysis revealed another missense variant rs146737847 (Glu129Lys) also in *SIX6* associated with VCDR ($P = 5.09 \times 10^{-3}$, $n = 1208$). These two findings point to *SIX6* as the responsible gene for the previously reported association signal. Functional characterization of *SIX6* in zebrafish revealed that knockdown of *six6b* led to a small eye phenotype. Histological analysis showed retinal lamination, implying an apparent normal development of the eye, but an underdeveloped lens, and reduced optic nerve diameter. Expression analysis of morphants at 3 dpf showed a 5.5-fold up-regulation of *cdkn2b*, a cyclin-dependent kinase inhibitor, involved in cell cycle regulation and previously associated with VCDR and POAG in genome-wide association studies (GWASs). Since both *six6b* and *cdkn2b* play a key role in cell proliferation, we assessed the proliferative activity in the eye of morphants and found an alteration in the proliferative pattern of retinal cells. Our findings in humans and zebrafish suggest a functional involvement of *six6b* in early eye development, and open new insights into the genetic architecture of POAG.

INTRODUCTION

Primary open-angle glaucoma (POAG) is a neurodegenerative disease (1) characterized by loss of retinal ganglion cells, optic nerve degeneration, and as a consequence, visual field loss and eventually blindness. It is recognized as a complex disease in which multiple genetic and environmental factors interact (2–4). Known risk factors include age, race, myopia, high intraocular pressure (IOP), decreased central corneal thickness and positive family history (1). First degree relatives of affected individuals are estimated to have a 10-fold increased risk of POAG compared with the general population (5). Heritability

*To whom correspondence should be addressed at: Department of Epidemiology, Erasmus Medical Center, PO Box 2040, 3000 CA Rotterdam, The Netherlands. Tel: +31-10-7043-394; Fax: +31-10-7044-657; Email: c.vanduijn@erasmusmc.nl
†These two authors contributed equally as senior authors.

estimates of related quantitative traits as optic disc area (ODA), vertical cup–disc ratio (VCDR), IOP and central corneal thickness are high (52–59%; 48–80%; 35–42% and 68–72%, respectively (6–9)).

Developments in the field of genomics have opened opportunities to uncover the genetic mechanisms involved in POAG. To date, at least 20 genetic loci have been linked to POAG, including three causative genes (*MYOC, OPTN*, *WDR36)* (10–12). In addition, genome-wide association studies (GWASs) have allowed the identification of candidate genes, such as *CAV1/CAV2* (13,14), which are expressed in the trabecular meshwork as well as in retinal ganglion cells, and *TMCO1* which is also expressed in retinal ganglion cells (15).

As in other disorders, GWAS of POAG have targeted on endophenotypes, i.e. heritable quantitative determinants of POAG. This approach has facilitated the identification of genes that were subsequently implicated in POAG. Three of the six loci that have been associated with neurodegeneration of the optic nerve (VCDR) (16) were also associated with POAG (17). The strongest associations were seen for the single-nucleotide polymorphism (SNP) rs1900004, within 10 kb of the *ATOH7* gene; the rs10483727 near *SIX1-SIX6* genes and the rs1063192, in the 3′UTR region of *CDKN2B* gene.

Two of these variants point to pathways involved in growth and development of the optic nerve. *ATOH7* and *SIX1–SIX6* genes are transcription factors involved in eye development (18–22). The role of *ATOH7* in eye development and retinal ganglion cell differentiation has been well characterized in several animal models (18–20). *SIX1* and *SIX6* are homeoprotein members of the SIX/sine oculis family of homeobox transcription factors (22). *SIX1* is highly expressed in skeletal muscle (23) and has been involved in myogenesis (24), while *SIX6* is highly expressed in the developing eye (25,26). To date, it is not clear which one of the two genes is causally related to optic nerve degeneration and POAG, asking for a more in-depth analysis of the *SIX1–SIX6* region.

The protein encoded by *CDKN2B* gene, the third POAG gene identified by GWAS of VCDR, has emerged as a key protein in the pathogenesis of optic nerve degeneration and POAG in different populations (15–17,27–33). *CDKN2B* gene is a member of the family of cyclin-dependent kinase (CDK) inhibitors which play a role in cell cycle regulation, influencing the proliferation/differentiation balance (34). In the *Six6* null mice it was demonstrated that *Six6* repress the transcription of members of the *Cdkn1* family, particularly *Cdkn1b* (35). Therefore, it may be speculated that the *SIX1–SIX6* region is potentially related to the *CDKN2B* regulation, although this has not been described.

In this study, we investigated the *SIX1–SIX6* locus in depth in human and zebrafish. First, we fine-mapped the region and performed a conditional, and exome sequencing analysis. As we found two variants that pointed to *SIX6* as best candidate gene, we next characterized the effect of *six6b* knockdown on eye development of zebrafish and evaluated expression levels of several target genes in morphants, including *cdkn2b*.

RESULTS

Fine mapping of the *SIX1–SIX6* region

The results of the analyses in the Rotterdam Study (RS) and the Erasmus Rucphen Family (ERF) study are shown in Table 1. The IOP analysis included 5782 (RS-I), 2116 (RS-II), 2038 (RS-III) and 2589 (ERF) participants. The optic nerve head analyses included 5322 (RS-I), 2054 (RS-II), 1966 (RS-III) and 2131 (ERF) participants with reliable data. The case–control studies consisted of 188 cases and 5548 controls from the RS-I and 104 cases and 2126 controls from the GRIP/ERF study.

Fine mapping of the *SIX1–SIX6* region based on imputations of the SNPs using 1000 Genomes Project revealed a missense variant rs33912345 in *SIX6,* this variant is in complete linkage disequilibrium with the previous reported intergenic variant rs10483727 (the two *D'* and $r^2 = 1$). Both the rs10483727 and the missense variant in *SIX6* rs33912345 were associated with VCDR ($P_{meta} = 5.56 \times 10^{-7}$ and 7.74×10^{-07}, respectively), ODA ($P_{meta} = 1.69 \times 10^{-3}$ and 3.51×10^{-3}, respectively) and POAG ($P_{meta} = 2.95 \times 10^{-3}$ and 6.09×10^{-3}, respectively) (see Table 1). The significant association between rs10483727 and VCDR disappeared after adjustment for rs33912345 ($P_{meta} = 8.72 \times 10^{-1}$), indicating that the *SIX6* variant is most likely responsible for the association. This variant determines an amino acid change (His141Asn) in the homeobox DNA-binding domain of *SIX6*. PolyPhen-2 (36) predicted a benign effect (score = 0) for this evolutionarily conserved variant, based on the Genomic Evolutionary Rate Profiling (GERP) (37) score = 5.38. No significant association was found with variants in *SIX1*.

Exome sequencing of *SIX1–SIX6* region

To determine whether there were other unobserved rare variants in *SIX6*, we explored the presence of exonic variants associated with VCDR in this region. In exome sequence data from 1208 individuals of the ERF study, we found another missense variant, rs146737847 (MAF = 0.0023), in *SIX6* ($P = 1.25 \times 10^{-3}$). This evolutionarily conserved variant (GERP = 5.38) determines an amino acid change (Glu129Lys) in the homeobox DNA-binding domain of *SIX6*, which PolyPhen-2 predicted as probably damaging (score = 0.971). When conducting a conditional analysis on rs33912345, the rs146737847 variant remained associated with VCDR ($P = 4.58 \times 10^{-3}$), confirming that both variants are independent of each other. Direction of the effect of both variants was the same; rs33912345 ($\beta = 0.011$, se = 0.002) and rs146737847 ($\beta = 0.183$, se = 0.055). No exonic variants in *SIX1* were significantly associated with VCDR

eQTL and expression analyses

No significant *cis* or *trans*-eQTLs effects for rs10483727, rs33912345 or rs14673784 were found in the GTEx project database (38). The Ocular Tissue Database (39) was used to compared the expression levels of *SIX1* and *SIX6* in different human ocular tissues. We found that *SIX6* is highly expressed in relevant tissues for POAG, including cornea, optic nerve, trabecular meshwork and retina, compared with *SIX1* (PLIER number 27.33 versus 9.65; 22.25 versus 18.32; 25.80 versus 15.43 and 26.08 versus 14.73; respectively).

Exclusion of an eQTL effect of the evaluated SNPs on the gene expression of *SIX1* or *SIX6,* together with the fine-mapping and exome sequencing data, suggests that the variants in *SIX6* rather

Table 1. Evidence of association of *SIX6* with VCDR and POAG in RS and ERF

	MA	RS-I MAF	β	SE	*P*	RS-II MAF	β	SE	*P*	RS-III MAF	β	SE	*P*	ERF MAF	β	SE	*P*	Meta-analysis β	SE	*P*-meta
IOP (~ age, sex, PC1, PC2)																				
rs33912345	C	0.41	0.034	0.064	5.8×10^{-01}	0.40	−0.039	0.096	6.8×10^{-01}	0.39	−0.070	0.093	4.5×10^{-01}	0.45	−0.251	0.087	4.1×10^{-03}	−0.062	0.041	1.3×10^{-01}
rs10483727	T	0.41	0.035	0.064	5.8×10^{-01}	0.40	−0.037	0.096	7.0×10^{-01}	0.39	−0.066	0.093	4.8×10^{-01}	0.44	−0.303	0.106	4.3×10^{-03}	−0.054	0.042	2.0×10^{-01}
DA (~ age, sex, PC1, PC2)																				
rs33912345	C	0.41	−0.020	0.009	3.2×10^{-02}	0.40	−0.031	0.015	3.4×10^{-02}	0.39	−0.019	0.014	1.6×10^{-01}	0.46	−0.003	0.011	8.0×10^{-01}	−0.017	0.006	3.5×10^{-03}
rs10483727	T	0.41	−0.020	0.009	2.7×10^{-02}	0.40	−0.033	0.015	2.6×10^{-02}	0.39	−0.018	0.014	1.7×10^{-01}	0.45	−0.006	0.014	6.5×10^{-01}	−0.019	0.006	1.7×10^{-03}
VCDR (~ age, sex, PC1, PC2)																				
rs33912345	C	0.41	0.013	0.003	4.2×10^{-07}	0.40	0.008	0.004	4.5×10^{-02}	0.39	0.002	0.007	7.8×10^{-01}	0.46	0.014	0.007	3.7×10^{-02}	0.011	0.002	7.7×10^{-07}
rs10483727	T	0.41	0.013	0.003	3.1×10^{-07}	0.40	0.009	0.004	3.1×10^{-02}	0.39	0.001	0.007	8.4×10^{-01}	0.45	0.017	0.008	3.5×10^{-02}	0.011	0.002	5.6×10^{-07}
VCDR (~ age, sex, PC1, PC2, spherical equivalent)																				
rs33912345	C	0.41	0.013	0.003	2.9×10^{-07}	0.40	0.009	0.004	2.6×10^{-02}	0.39	0.001	0.007	9.1×10^{-01}	0.46	0.014	0.007	3.7×10^{-02}	0.011	0.002	4.8×10^{-07}
rs10483727	T	0.41	0.013	0.003	2.2×10^{-07}	0.40	0.010	0.004	1.8×10^{-02}	0.39	0.000	0.007	9.7×10^{-01}	0.45	0.017	0.008	3.5×10^{-02}	0.011	0.002	3.5×10^{-07}
VCDR (~ age, sex, PC1, PC2, rs33912345)																				
rs10483727	T	0.41	0.000	0.003	9.3×10^{-01}	0.40	0.001	0.004	8.7×10^{-01}	0.39	0.000	0.007	9.4×10^{-01}	0.44	0.001	0.008	9.3×10^{-01}	0.000	0.002	8.7×10^{-01}
POAG (~ age, sex, PC1, PC2)																				
rs33912345	C	0.41	0.252	0.106	1.8×10^{-02}	NA	NA	NA	NA	NA	NA	NA	NA	0.46	0.230	0.164	1.6×10^{-01}	0.244	0.089	6.1×10^{-03}
rs10483727	T	0.41	0.246	0.106	2.0×10^{-02}	NA	NA	NA	NA	NA	NA	NA	NA	0.45	0.379	0.194	5.1×10^{-02}	0.277	0.093	2.9×10^{-03}

than *SIX1* explain the observed association signal reported in previous studies in the region.

Identification and characterization of zebrafish *six6b*

A zebrafish six6 ortholog was retrieved from the Ensembl database. Two genes were found, *six6a* and *six6b*. The protein encoded by *six6a* together with the protein encoded by *six6b* was blasted against the human *SIX6* protein, showing that *six6a* and *six6b* independently have 91% identity to the human *SIX6*, while the overall identity of both zebrafish *six6* to the human protein is 88% (Supplementary Material, Fig. S1). In this study, we evaluated the effect of *six6b* depletion.

To evaluate the role of *six6b* at different time points of the development, a quantitative reverse transcription PCR (RT-qPCR) was performed. Taking reference expression levels at 1 day post fertilization, we found that over time expression of *six6b* gradually increases, reaching a peak at the larvae stage of 3 dpf, then decreasing at 5 dpf (Fig. 3A).

six6b is required for normal eye development in zebrafish

To evaluate the function of *six6b* during embryonic development, two non-overlapping antisense MOs were designed, the first one targeting the AUG translation initiation site (*six6b* AUG-MO) and the other targeting the exon1/intron1 splice site (*six6b* SB-MO). Since embryos injected with either *six6b* AUG-MO or *six6b* SB-MO developed similar dose-dependent (2–12 ng) small eye size compared with controls, the *six6b* SB-MO (6 ng) was selected for further studies as it provided the possibility of quantifying the efficiency of knockdown by RT-qPCR. Embryos injected with the highest concentration of the MOs (12 ng) showed a severe phenotype (twisted trunk, small head and eye, massive heart edema and lethality at ~4 dpf, data not shown).

Eye size difference between injected and control embryos was quantified at 5 dpf since the phenotype is then well defined and easy to evaluate (Fig. 1A). Seventy-eight percent of the injected embryos showed a small eye phenotype ($n = 286$). RT-qPCR analysis indicated *six6b* SB-MO reduced *six6b* mRNA levels by 70% (Supplementary Material, Fig. S2). To elucidate whether morphants showed small eye phenotype secondary to *six6b* knockdown as opposed to an overall delay in development, we measured the ratio of the eye size to body length (E:B) (40). The E:B ratio was measured in 30 embryos of each group (Fig. 1B). Morphants showed small eyes compared with controls, suggesting an eye development delay (mean E:B = 0.064 versus 0.092, $P = 4.96 \times 10^{-20}$). Other abnormalities were observed as pericardial edema, diffuse pigmentation that resembles an expanded melanophore phenotype, small head, and in some embryos short jaw. To exclude the presence of small head as a principal cause of a small eye, we measured the ratio of the eye size to head length (E:H) in ~30 embryos of each group (i.e. wild-type (WT), *six6b* SB-MO injected and *six6b* SB-MO + *p53*-MO co injected). This measure provides the possibility of evaluating the impact of *six6b* knockdown on eye size independent of the head size reduction. The E:H ratio was significantly smaller in morphants compared with WT embryos (mean E:H = 0.445 versus 0.530, $P = 2.59 \times 10^{-10}$; Supplementary Material, Fig. S3).

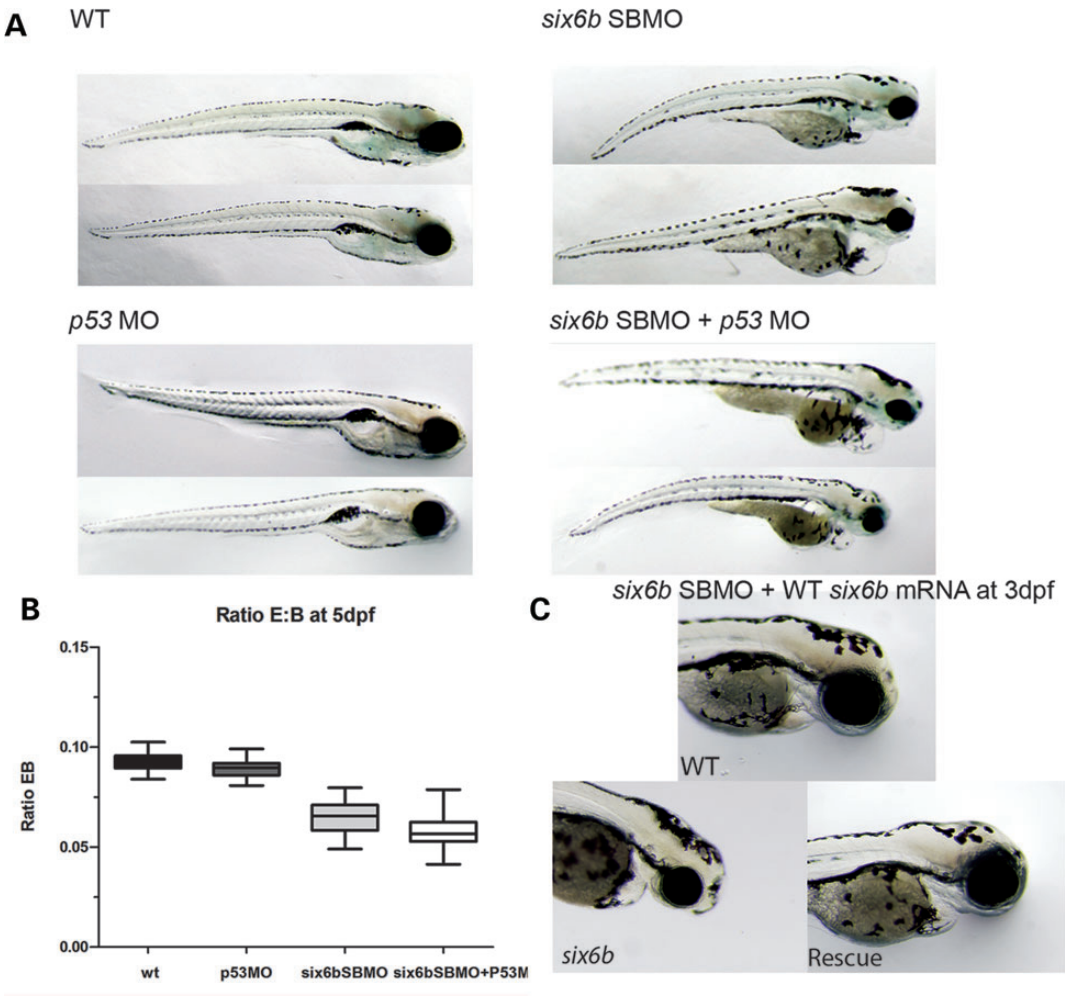

Figure 1. Phenotype characterization of *six6b* SB-MO injected fish. (**A**) *six6b* knockdown results in a small eye phenotype, other abnormalities including pericardial edema, diffused pigmentation small head and short jaw were also observed. The small eye phenotype was not rescued after co-injection with *p53*-MO indicating a specific effect of *six6b* SB-MO on eye size. (**B**) Ratio of eye to body size (E:B) in morphants and *p53* co-injected compared with WT embryos, $n = 30$ for each group. *P*-values are indicated in the text. (**C**) Co-injection of wt *six6b* mRNA and *six6b* SB-MO partially rescued the small eye phenotype. The mean eye area improves from 1.425.747 to 1.749.203 μm^2, $P = 0.001$.

We performed two control experiments; first, a specific *p53*-targeting MO (4 ng) was co-injected with the *six6b* SB-MO (6 ng) to exclude whether the phenotype observed was due to off-target effects mediated by induction of *p53* expression. The mean ratio E:B in *p53*-MO co-injected embryos was 0.061, showing a small eye phenotype comparable with *six6b* knockdown ($P = 2.41 \times 10^{-31}$). Excluding a small eye size as a consequence of *p53*-mediated apoptosis pathway. Second, we conducted rescue experiments using WT *six6b* mRNA. Since no difference in the body length was observed between WT and morphants at 5 dpf (mean = 3.952 mm versus 3.908 mm, respectively; $P = 1.95 \times 10^{-1}$), assessment of rescue experiments was focused on eye dimensions only. Co-injection of *six6b* SB-MO with wt-*six6b* mRNA resulted in a partial, but significant, rescue of small eye phenotype (mean eye area improved from 1.425.747to 1.749.203 μm^2, $P = 1 \times 10^{-3}$; Fig. 1C and Supplementary Material, Fig. S4).

Loss of *six6b* results in immature and underdeveloped eyes

In order to carry out detailed assessment of the *six6b* SB-MO small eye phenotype, histological analysis was performed on embryos at 3 and 5 dpf (Fig. 2A–G). Histology revealed that retinal lamination in morphants occurred. Therefore, the ganglion cell layer (GCL), inner nuclear layer (INL), and outer nuclear layer (ONL) were visualized by H&E staining. Although the optic nerve was seen leaving the retina, its thickness was decreased compared with WT embryos. A semi-quantitative analysis on serial sections of six microns showed that the optic nerve thickness on WT embryos ($n = 4$) was around 21 μm, while in morphants ($n = 4$) it was ~12 μm. In addition, the lens of 3 dpf morphants was immature and cellularized compared with controls of the same age, supporting that eyes of morphants were delayed in development. Eyes of morphants at 5 dpf showed a conserved general architecture, leaving small size as

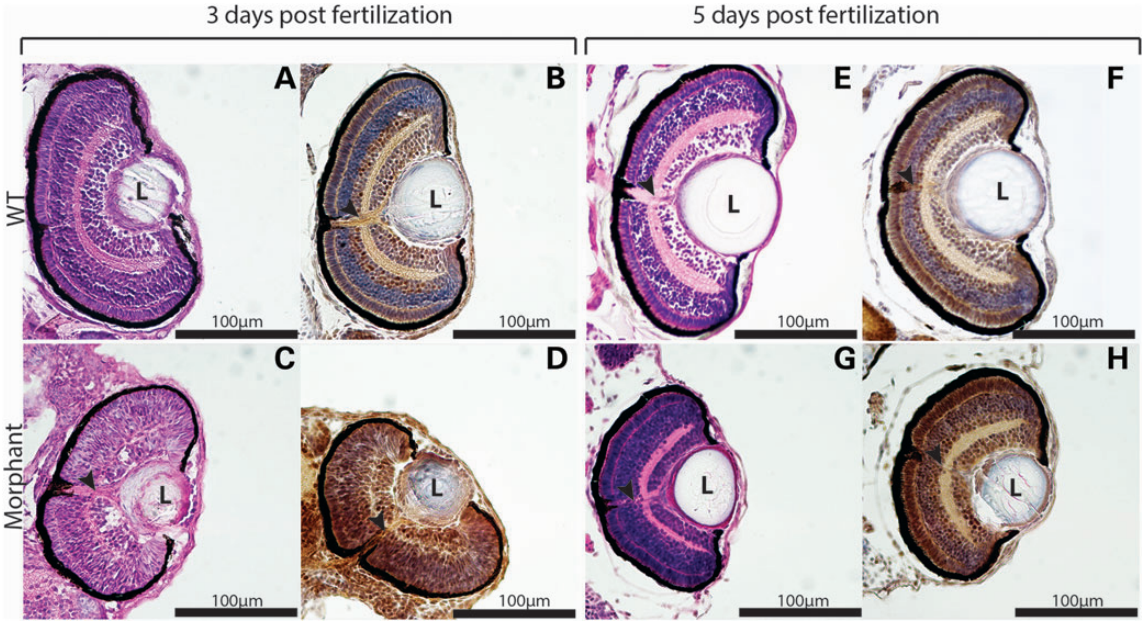

Figure 2. *six6b* knockdown results in small and underdeveloped eyes. (**A**–**D**) Representative images of histological sections of WT (A and B) and morphants (C and D) at 3 dpf. Though retinal lamination occurred in morphants, note the cellularized and underdeveloped lens. Panels (A) and (C) were hematoxylin–eosin (H&E) stained. (**E**–**H**) Histological sections of WT (E and F) and morphants (G and H) at 5 dpf. Note that at this age small eye size was the principal difference between the groups, the lens of morphants resembles the WT lens. Panels (B, D, F and H) show immunohistochemical localization of *six6/six3* in both WT and morphants. The optic nerve is marked by arrowheads; L = Lens.

the principal difference between control embryos and morphants at this age.

Immunohistochemical localization of *six6* was studied using a rabbit anti-SIX6 polyclonal antibody on sections at 3 and 5 dpf (Fig. 2B–H). Since the rabbit anti-SIX6 can recognize the protein products of the closely related *six3a* and *six3b* as well, the anti-SIX6 immunoreactivity was only used to investigate the localization of *six6/3* proteins in the zebrafish retina, not for the efficiency of *six6b* knockdown. Both WT and morphants were analyzed. Consistent with previous studies in chick embryos, mouse, and human fetal and adult eye (21,22,41–43), we found *six6/3* protein localized in the nuclei of the GCL, the nuclei of potential bipolar, amacrine and horizontal cells located in the INL, the nuclei of the photoreceptors and the optic nerve (Fig. 2B–F). In general, labeling in WT embryos at 3 dpf was stronger than at 5 dpf. Morphants at 3 dpf presented less intense labeling, as predicted from expression data.

Expression patterns of *six3a* and *six3b* in *six6b* morphants

The *SIX* gene family of homeoproteins is required in both *Drosophila* and vertebrates for eye development. Similar to *SIX6*, *SIX3* has also been involved in eye development (26,44–46), both genes share high homology and are expressed during early stages (21,25). To determine whether zebrafish *six3* can compensate *six6b* depletion, RT-qPCR of morphants at 3 dpf was performed. Two orthologs of the human *SIX3* were retrieved from Ensembl, *six3a* (ENSDARG00000058008) and *six3b* (ENSDARG00000054879). RT-qPCR of morphants compared with WT showed an expected down-regulation of *six6b*. Surprisingly, we found down-regulation of *six3a* in morphants as well, while expression levels of *six3b* were not significantly deregulated (Fig. 3B).

Knockdown of *six6b* up-regulate expression of the cell cycle inhibitor *cdkn2b* in zebrafish

Since *Six6*/*Dach* interacts with some members of the family of cyclin-dependent kinases (CDK) inhibitors (35), we decided to evaluate whether knockdown of *six6b* in zebrafish alters the expression of *cdkn2b*, another member of the CDK inhibitors previously associated in our GWAS studies with VCDR (16) and POAG (17). RT-qPCR was performed at 3 dpf on injected and WT embryos, showing a 5.5-fold overexpression of *cdkn2b* in morphants compared with WT ($P = 1.56 \times 10^{-02}$), while *cdkn2c* and *cdkn2d* (taken as a control) remain unaffected (Fig. 3C). Expression levels of *dacha* and *dachb* at 3 dpf showed no differences between morphants and controls (data not shown).

Effect of *six6b* knockdown on cell proliferation in the developing eye of zebrafish

To evaluate whether up-regulation of *cdkn2b* in morphants leads to premature cell cycle exit, we examined the expression of the proliferating cell nuclear antigen (PCNA) in eye by immunostaining. WT embryos and morphants at 2, 3, 4 and 5 dpf were analyzed.

In WT fish at 2 dpf, almost all retinal progenitor cells showed a strong PCNA immunoreactivity (Fig. 4A). As expected, in WT embryos at 3, 4 and 5 dpf, cells concentrated in the ciliary marginal zone were PCNA-positive (Fig. 4B–D). The ciliary marginal zone is a proliferative zone described in eye of cold-blooded vertebrates (47). Thus, this finding is consistent with normal retinal differentiation processes in zebrafish (48,49). In contrast, morphants at 3 and 4 dpf showed numerous PCNA-

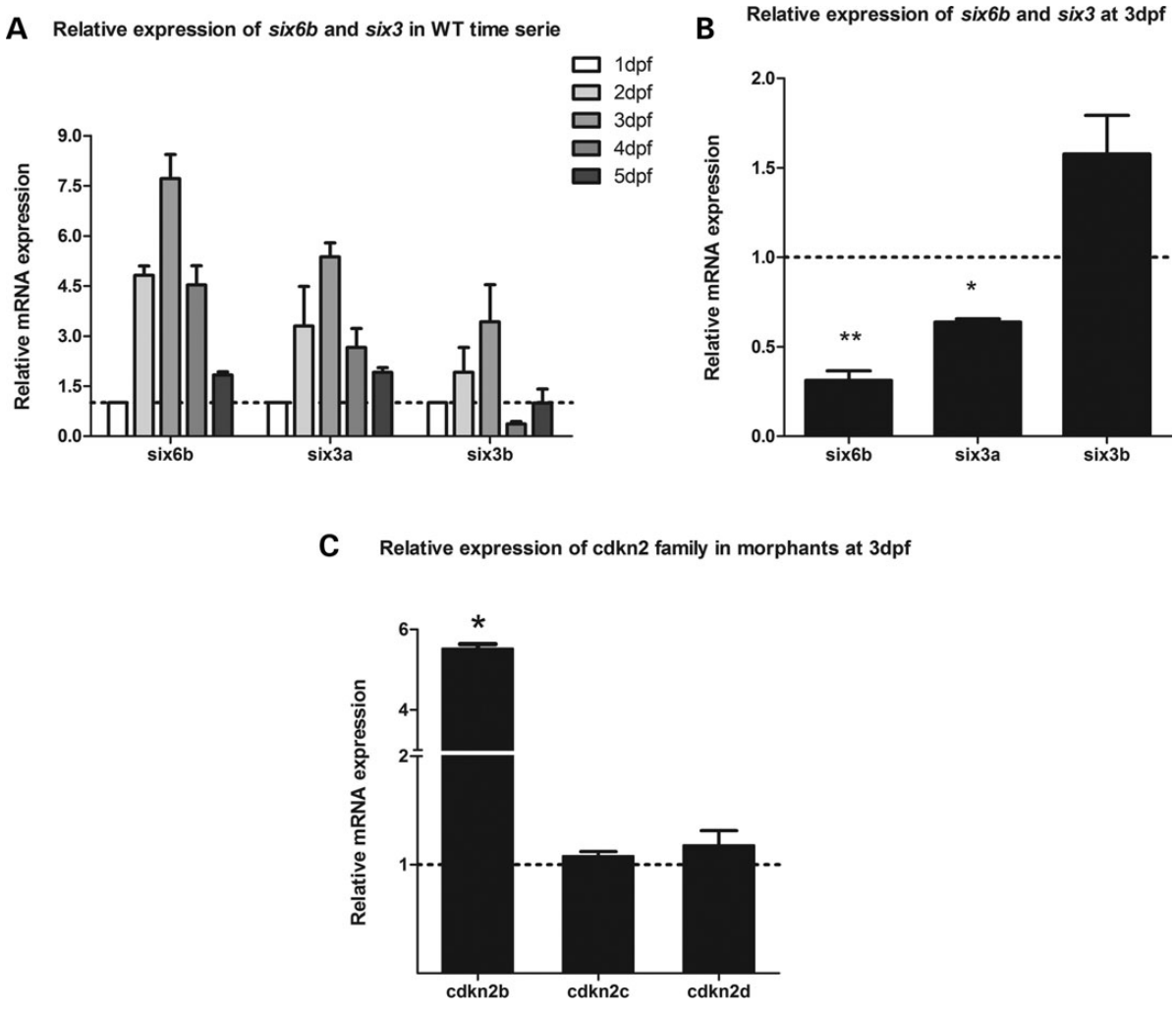

Figure 3. *six6*, *six3a/six3b* and *cdkn2b* mRNA expression change. (**A**) WT relative expression of *six6b*, *six3a* and *six3b* over time from 1 to 5 dpf. Relative expression was calculated by setting the 1 dpf expression level at 1. Samples expression were normalized to the control gene *β-actin* (**B**) *six6b* knockdown in response to *six6b* SB-MO at 3 dpf. In addition, morphants showed downregulation of *six3a* but no *six3b* (**C**) Overexpression of *cdkn2b* in response to *six6b* depletion. All sample expression from experiments B and C were normalized to the control gene *sdha*. Relative expression was calculated by setting the WT expression level at 1. Values represent means ± s.e.m. $^{*}P < 0.05$; $^{**}P < 0.01$.

positive cells in the photoreceptor and inner nuclear layers (Fig. 4F and G), suggesting that proliferation in morphants was not restricted to the ciliary marginal zone; on the contrary, retinas of morphants at 3 and 4 dpf showed a PCNA immunoreactivity pattern that resembled 2 dpf WT retinas. At 5 dpf morphants showed PCNA immunoreactivity mostly restricted to the ciliary marginal zone comparable with WT embryos (Fig. 4H). We also investigated whether increased apoptosis was the cause of small eye phenotype. Caspase-3 staining did not show an increased apoptosis rate in morphants compared with WT embryos (Supplementary Material, Fig. S5).

DISCUSSION

In this study, we investigated the *SIX1–SIX6* region in more detail to understand its role in optic nerve degeneration. Fine mapping and conditional analysis revealed a missense variant, rs33912345, in the *SIX6* gene. Further analysis of the *SIX6* exonic region revealed another rare missense variant, rs146737847. Both variants are located in the homeobox DNA-binding domain of *SIX6* and are highly evolutionarily conserved. No common or rare variants in *SIX1* were significantly associated to VCDR or POAG.

In line with previous findings, the rs33912345 has been described in patients with severe eye malformations, including anophthalmia, microphthalmia and coloboma (22,50,51). It is in complete linkage disequilibrium with the reported SNP rs10483727, which is known to be associated with VCDR and POAG (16,17,30). The rs146737847 variant has been reported in POAG cases of United States at the American Society of Human Genetics meeting 2012 (http://www.ashg.org/2012meeting/abstracts/fulltext/f120122353.htm).

SIX6 in adult human tissues is highly expressed in the choroid, ciliary body, sclera, optic nerve head and retina, particularly GCL, INL and ONL (43). Mouse, chick and *Xenopus* studies have demonstrated a role of *Six6* during eye development (22,26,35,52), whereas *Six1* is highly expressed in skeletal

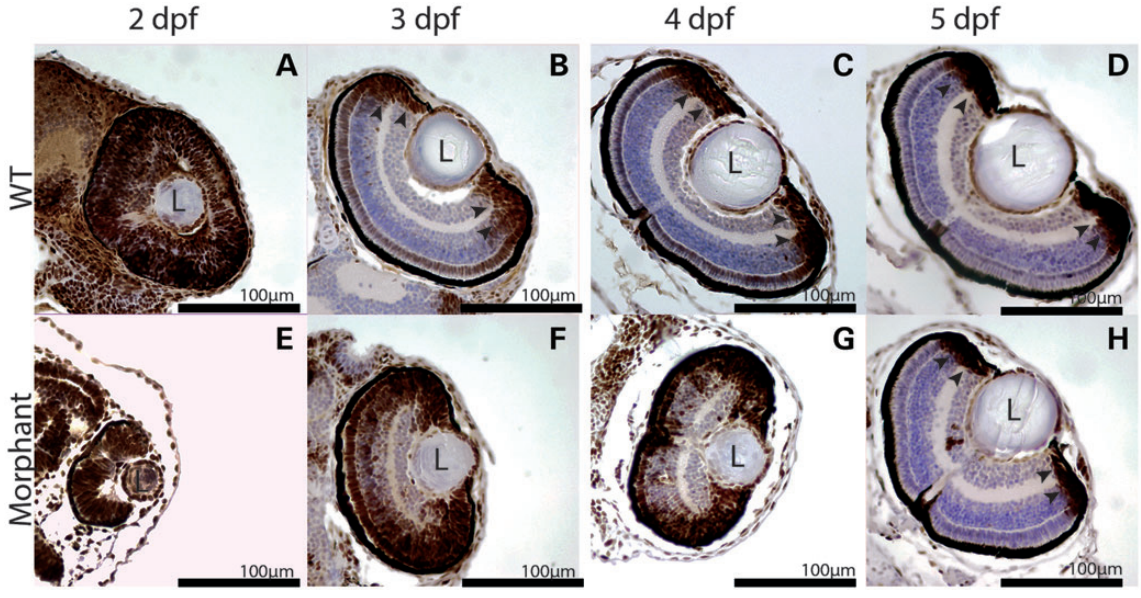

Figure 4. *six6b* is involved in proliferation and differentiation of retinal cells in zebrafish. (**A**–**D**) Representative images of PCNA immunoreactivity in WT embryos at 2, 3, 4 and 5 dpf; (A) In WT embryos at 2 dpf almost all cells were PCNA-positive, the lens was cellularized and there was not retinal lamination, while at 3, 4 and 5 dpf (B–D) proliferation is restricted to the ciliary marginal zone, marked by arrowheads. Retinal lamination is clear and the lens is mature and not cellularized. In contrast, morphants at 3 and 4 dpf present proliferating cells located outside the ciliary marginal zone (**F** and **G**). Note that at 5 dpf the morphants resembles the WT retina, although some cells located in the central retinal showed a positive PCNA signal (**H**).

muscle (23) and plays a role in myogenesis (24). Both our findings and the known biological function support the notion that *SIX6,* rather than *SIX1,* may play a role in VCDR and POAG.

To evaluate the function of the *SIX6* gene on eye development and POAG. We used zebrafish as animal model due to its numerous advantages in comparison to mammalian models (53). We assessed the effect of *six6b* knockdown in zebrafish. Deficiency of *six6b* in zebrafish led to a small eye phenotype, associated with small head and pericardial edema. Although morphants showed a small head, we found that the eye of morphants remains smaller independently of the head size. Other abnormalities, including diffused pigmentation were also observed. A clear connection between the visual system, particularly retinal-hypothalamic projections, and the control of pigment cells has been established (54–56). In this study, *six6b* depleted embryos showed diffused pigmentation, a feature present in mutants who lack the ability to sense ambient light (57). This may indicate an abnormal eye function in *six6b* morphants. Furthermore, histological sections of *six6b* morphants at 3 dpf showed a rudimentary lens, which indicates a developmental delay of the eye. Also, the optic nerve had a reduced thickness when compared with age-matched controls, which is relevant in the context of the neurodegenerative disease POAG. This finding is consistent with previous analysis of *Six6* null mice (35), which showed retinal hypoplasia, with often absence of optic nerve and chiasm. All these results support our hypothesis that the main effect of *six6b* knockdown is in the ocular system.

In flies, *sine oculis* (*so*) and *Optix* play a central role in eye development (25,58). In vertebrates, the *Six3* and *Six6* are the homologs of *Optix*. Both the *Six3* and *Six6* show high homology and are expressed during early stages of eye development (25,26). *Six3* has a wide role in forebrain development, whereas *Six6* has a more specific role in eye development (35,45,46,52,59–61). We evaluated the effect of *six6b* knockdown on expression levels of *six3a* and *six3b*. No significant changes in expression levels of *six3b* were found in morphants compared with WT embryos. Interestingly, we found down-regulation of *six3a* in *six6b* morphants. However, 14 mismatches between the *six6b* SB-MO and the *six3a* gene confirmed that our MO did not target *six3a*. Down-regulation of *six3a* in *six6b* morphants might suggest a complex feedback mechanism between *six3a/six3b* and *six6b* in zebrafish. Though both *Six3* and *Six6* might function through similar (62) and different (63) mechanisms, our results show that in zebrafish *six6b* is needed for normal eye development. Neither *six3a* nor *six3b* can compensate for *six6b* deficiency, resulting in a small eye phenotype.

Studies in medaka fish indicate that *Six3* and the replication–initiation inhibitor *gemini* act antagonistically to regulate the balance between proliferation and differentiation during eye development (62). *Six6* also interacts with *gemini* (62), supporting a potential role of *Six6* in cell proliferation and differentiation. Additionally, in the *Six6* null mice it was demonstrated that *Six6* interacts with *Dach1*, a transcriptional co-repressor, to suppress *Cdkn1b* transcription *in vivo* (35). *Cdkn1b* is a member of the CDK inhibitor family and controls the cell cycle progression, arresting cell proliferation. *CDKN2B,* a gene known to be associated with VCDR and POAG (16,17,27,28,30,64), is also a member of the CDK inhibitor family. *CDKN2B* controls G1 progression of the cell cycle and is highly induced by *TGF-β* (65), which in turn is one of the pathways involved in POAG pathogenesis (17). We demonstrated a 5.5-fold overexpression of *cdkn2b* in *six6b* morphants compared with WT embryos. This finding is in accordance with a rat model of glaucoma (15), in which overexpression of *Cdkn2b* was described after induction of high IOP. Up-regulation of *cdkn2b* arrests cell cycle progression causing an abnormal proliferation and small eye phenotype.

Based on our results, we conclude that *Six6* repress the expression not only of *Cdkn1b,* as previously reported (35), but also *cdkn2b*. This reveals a new interaction between the two known pathways associated with POAG (developmental and *TGF-β* signaling pathways) (Fig. 5A; www.ingenuity.com).

Next, we evaluated the proliferative activity of retinal cells through PCNA assessment. PCNA allows detection of cells in either G1 or S phase of the cell cycle. We found that knockdown of *six6b* changes the pattern of positive PCNA labeling. Similar results were found in a previous study, in which a collagen gene (*drCol15a1b*) was knockdown in zebrafish (66). It is well established that retinal progenitor cells start a differentiation process when they exit the cell cycle (66,67). Analysis of *drCol15a1b* morphants indicated that cells arrested in a proliferative state were undifferentiated (66). Our results demonstrate an abnormal proliferation in the presence of an efficient knockdown of *six6b* with a recovery at 5 dpf. This could be explained by a reduced morpholino activity, as a consequence of its dilution due to cell growth and division. Based on our findings, we hypothesized that decreased expression of *six6b* may lead to fewer differentiated cells as depicted by our proposed model in Figure 5B. This needs to be assessed in future studies by evaluating the presence of retinal-differentiated cells in the eyes of *six6b* morphants. *Caspase-3* assessment did not show an increased number of apoptotic cells in the eye of *six6b*-depleted embryos.

In conclusion, by combining fine-mapping and exome sequence analysis we found that *SIX6,* rather than *SIX1,* is responsible for the association signal previously reported in the *SIX1/SIX6* region. We found two variants located in the DNA-binding homeodomain of *SIX6*, which were significantly associated with VCDR. The rs33912345 variant was also associated with POAG in our study. Knockdown of *six6b* in zebrafish led to a small eye phenotype, as a result of an abnormal proliferative pattern in retinal cells. This alteration may also be associated with a disturbance in the differentiation process of retinal progenitor cells. Additionally, we were able to find an *in vivo* interaction between proteins identified by the GWAS (SIX6 and CDKN2B) for POAG. Further biological research is needed to verify the exact mechanism behind this interaction. Our findings from genetic association and functional studies demonstrate that *SIX6* is a susceptibility gene for POAG and is involved in early eye development. This study provides new insight into the complex genetic architecture of POAG.

MATERIALS AND METHODS

Human and fine-mapping studies

Study populations

The RS is a prospective cohort study in the district Ommoord of Rotterdam. The rationale and study design are described elsewhere (68). The original cohort (RS-I) consisted of 7983 residents aged ≥55 years. In 2000, the cohort was extended with 3011 residents aged ≥55 years (RS-II). In 2006, the cohort was further expanded with 3932 residents aged 45–54 years (RS-III). Details about examinations in each one of the cohorts are described elsewhere (16).

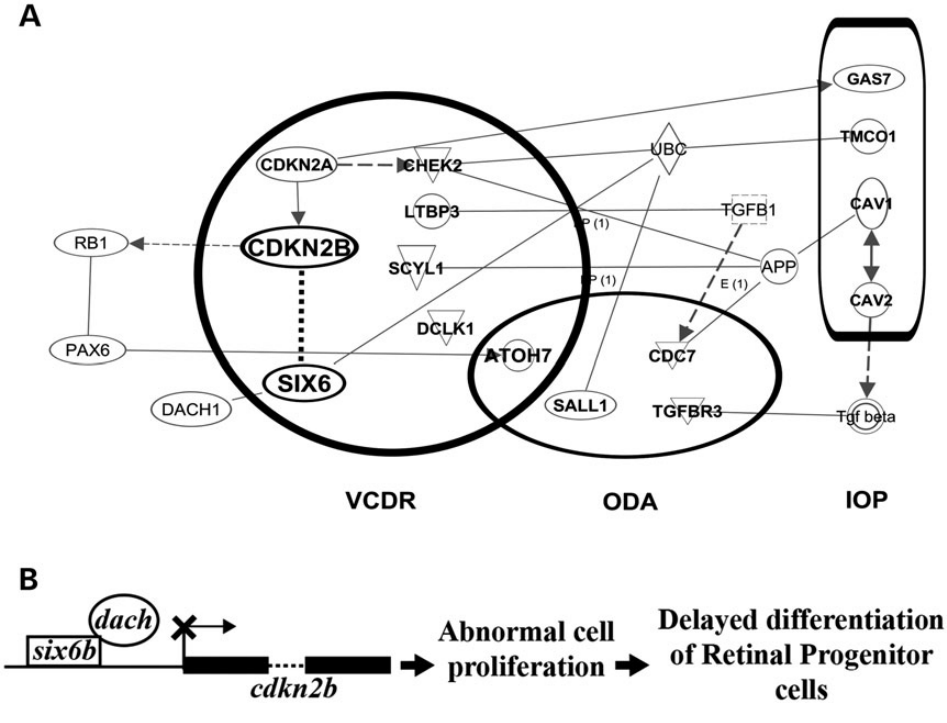

Figure 5. *six6b* and *cdkn2b* interaction. (**A**) Ingenuity diagram of the biological interaction of the known genes identified through the GWAS of optic disc parameters (VCDR, ODA and IOP); the bold dashed line shows the new interaction found in this study using a zebrafish model. The Ingenuity knowledge base is a repository of biological interactions and functional annotations of *in vivo* and *in vitro* experiments (www.ingenuity.com). The diagram was generated using the function 'Path Explorer'. (**B**) *six6b* represses *cdkn2b* transcription in association with the co-represor *dach. six6b* and *dach* form a complex that interacts with the regulatory region of *cdkn2b*. This interaction blocks *cdkn2b* transcription and thus controls the proliferative state of retinal progenitor cells. VCDR, vertical cup–disc ratio; ODA, optic disc area; IOP, intraocular pressure.

The ERF Study is a family-based study in a genetically isolated population in the southwest of the Netherlands. It includes over 3000 participants with age varying between 18 and 86 years old. The cross-sectional examinations took place between 2002 and 2005. The rationale and study design have been described elsewhere (69,70).

An independent series of 104 glaucoma cases from an isolated population (the Genetic Research in an Isolated Population [GRIP] study) was used for a case–control analysis. These patients were recruited in three local hospitals in the geographical region of the ERF study. They did not participate in the ERF study. Participants from the ERF study were used as the control population.

Ophthalmic examinations

The ophthalmic assessment in the RS and ERF study included a medical history, autorefraction, keratometry, IOP measurements, visual field testing, fundus photography and optic nerve head imaging. Details about IOP and optic disc measurements are described elsewhere (16,71). In RS-I, glaucoma diagnosis was based on glaucomatous visual field loss (GVFL). The visual field of each eye was screened using a 52-point supra-threshold test that covered the central visual field with a radius of 24°, and that tested the same locations as used in the Glaucoma Hemifield Test. Participants with a reproducible visual field loss in a second supra-threshold test, were evaluated with a Goldmann kinetic perimetry or full-threshold HFA test by a skilled perimetrist on both eyes. We incorporated prevalent glaucoma cases, (72) as well as incident cases (73) based on GVFL during at least one of the examination rounds. VCDR *per se* was not an inclusion criteria of the diagnosis. In GRIP/ERF, the diagnosis was based on the optic disc appearance, visual field testing and angle assessment.

The study protocols were approved by the Medical Ethics Committee of the Erasmus University, and all participants have given a written informed consent in accordance with the Declaration of Helsinki.

Genotyping and statistical analyses of fine-mapping studies

Illumina Infinium II HumanHap550 chip v3.0 array was used for DNA genotyping in RS-I, RS-II and RS-III. In the ERF study, genotyping was performed using Illumina 318 K, Illumina 370 K, Illumina 610 K and Affymetrix 250 K genotyping platforms. Imputation for both studies was done by using 1000 Genomes Phase 1 (v3) as the reference.

We used the mean IOP, VCDR or ODA of both eyes. In cases of missing or unreliable data on one eye, the other eye was taken. Participants with a history of glaucoma laser or surgery were excluded for the IOP analysis. IOP measurements of participants with IOP lowering medication were imputed by adding 25% to the value of the measurement. We used 1000 Genomes Phase 1(v3) to perform fine mapping and modeling of *SIX1/SIX6* locus in relation to these continuous outcomes on an assumed additive model for the effect of the risk allele. Additionally, we examined through logistic regression the association between the *SIX1/SIX6* locus and primary open-angle glaucoma. All analyses were adjusted for age, sex, the first two principal components (RS) or family structure (ERF). Extra adjustments were done with spherical equivalent, as a measure of myopia, to evaluate whether the missense variant rs33912345 was independently associated with VCDR. The spherical equivalent was calculated for each eye using the standard formula: spherical equivalent = sphere + 1/2 cylinder. Additionally, independence between rs10483727 and rs33912345 was tested, adjusting for the last one. Then, an inverse variance weighted meta-analysis was performed.

Exome sequencing

Exomes of 1309 individuals from the ERF population were sequenced 'in-house' at the Center for Biomics of the Cell Biology department of the Erasmus MC, The Netherlands, using the Aligent version V4 capture kit on an Illumina Hiseq2000 sequencer and the TrueSeq Version3 protocol. The sequences reads were aligned to the human genome build 19 (hg19) using Burrows-Wheeler Aligner (74) and NARWHAL pipeline (75). For each sample, at least 4 Gigabases of sequence was aligned to the genome with an average fold-coverage of 74.23x per base. Subsequently, the aligned reads were processed further using the Indel Realigner, Mark Duplicates and Table Recalibration tools from the Genome Analysis Toolkit (GATK) (76) and Picard (http: picard.sourceforge.net) to remove systematic biases and to recalibrate the PHRED quality scores in the alignments. Genetic variants were called using the Unified Genotyper Tool from GATK. Of the 1309 individuals, 1208 had data on VCDR. As the ERF study included related individuals, association analysis was performed in SOLAR using procedure 'polygenic –screen', and adjusting for age and sex. In total, two variants in *SIX1* and seven variants in *SIX6* with a call rate of >0.99 were found. Only one of the nine variants at *SIX6,* rs146737847, reached significance levels. In addition, conditional analyses were performed with the rs33912345, previously found in the fine-mapping analysis.

eQTL and expression analyses

We used the Genotype-Tissue expression (GTex) project database (www.broadinstitute.org/gtex/) to examine whether rs10483727, rs33912345 or rs146737847 had a *cis*- or *trans*-eQTL effect. Although the GTex database does not include eye tissues, it contains more than 10 different brain regions and other tissues. For *trans*-eQTL analysis, a *P*-value of 5×10^{-13} was considered significant (38).

Additionally, we compared expression levels of *SIX1* and *SIX6* using the Ocular Tissue Database (https://genome.uiowa.edu/otdb/). The gene expression is indicated as Affymetrix Probe Logarithmic Intensity Error (PLIER) number. The PLIER numbers were calculated by GC-background correction, PLIER normalization, log transformation and *z*-score calculation (39). Larger PLIER numbers represent high expression levels of a particular gene in particular tissue.

Statistical analysis of zebrafish experiments

Statistical analysis was performed using SPSS statistics 20. Analysis of E:B and E:H ratios was performed using the Student's *t*-test. Each group (*six6b* SB-MO injected, p*53* MO injected and *six6b* SB-MO + *p53* MO co-injected) was compared individually with the WT group ($n = 30$, in each group). All RT-qPCR experiments were undertaken in triplicate. Results were considered statistically significant when $P < 0.05$, and are denoted in the figures with an asterisk.

Zebrafish maintenance

The zebrafish (*Danio rerio*) strain used for this work was the Tupfel long fin (TL). Adults were maintained at 28°C on a 14 hour-light/10 h dark cycle. Embryos were collected from natural mating and raised in system water containing methylene blue at 28°C. Developmental stages were determined according to Kimmel (77). All procedures and conditions were in accordance with the Dutch animal welfare legislation. The use of zebrafish for this study was approved by the Institutional Review Board for experimental animals of the Erasmus MC, Rotterdam.

Genetic analysis of the zebrafish SIX6 *ortholog*

The zebrafish *six6* ortholog was retrieved from Ensembl using the comparative genomics tool (78). Two genes were found, *six6a* (ENSDARG00000025187) and *six6b* (ENSDARG00000031316). In this study, we reported the effect of *six6b* knockdown. We sequenced WT zebrafish *six6b* to corroborate the reference sequence and select the regions for morpholino oligonucleotide (MO) design.

Morpholino and mRNA microinjections

Morpholino antisense oligonucleotides were obtained from Gene-Tools (Philomath, OR, USA). Two morpholinos were designed against *six6b*. One morpholino was designed to target the translation initiation site: AUG-MO = 5′-AAATTGG CAACTGAAACATGAAGGC-3′; and the second morpholino targeted exon 1 donor site: SB-MO = 5′-TGTAAATCTGGAA AACGCACCTGTT-3′. All MO sequences were aligned with the Danio rerio genome using NCBI and UCSC Blast to confirm specificity to the *six6b* genomic region and ratify that neither the AUG-MO nor the SB-MO recognized *six6a, six3a* or *six3b*. A previously described MO designed to target the translation site of *p53* (p53-MO = 5′-GCGCCATTGCTTTGC AAGAATTG-3′ was used for control experiments (79). Morpholinos were reconstituted in distilled water and further diluted in Danieau solution containing 0.1% Phenol Red for microinjections into embryos.

Indicated dosages of MOs were injected into the yolk of one to two cell stage using a pneumatic picopump (World Precision Instruments, Berlin, Germany). Optimum dose was considered when maximal knockdown efficiency, low mortality rate and small eye phenotype without severe malformations were observed on injected embryos. Six nanograms of either SB or AUG-MO were selected as optimal concentration. In separate experiments, 4 ng of *p53*-MO was co-injected with 6 ng of *six6b*-specific MO (SB or AUG), in order to detect off-target effects due to activation of *p53* expression.

For MO rescue experiments, WT Danio rerio *six6b* cDNA was ligated into the pCR2.1-TOPO vector (Invitrogen), and subcloned at the site of *Eco*RI in pCS2+ vector. The fidelity of *six6b*-pCS2 was verified by direct sequencing. Using as template *Nsi*I linearized *six6b*-pCS2, WT *six6b* mRNA was synthesized using a mMESSAGE mMACHINE SP6 kit (Ambion Inc). Double injection of mRNA and MO was carried out in two steps, first 3 ng *six6b* SB-MO were injected into the yolk, then a second injection with 9 pg *six6b* mRNA into the cell was performed, all embryos were injected in one-cell stage. Eye size was evaluated at 3 dpf.

RNA isolation and RT-qPCR

Pooled embryos were snap frozen in liquid nitrogen and stored at −80°C. Total RNA from ∼60 WT embryos at 1,2,3,4 and 5 dpf was isolated for time series analyses. For evaluation of *six6b* knockdown, total RNA was isolated from ∼60 morphants and WT embryos at 3 dpf; in all extractions an RNA-Bee (Tri-Test, Inc) protocol was used. Synthesis of cDNA was performed using Superscript III reverse transcriptase (Invitrogen, CA, USA). To measure mRNA levels, qRT-PCR on cDNA samples was carried out using an SYBR® select Master Mix for CFX (Applied Biosystems, Inc., USA). All samples were analyzed on the Bio-Rad CFX96 qPCR detection system.

Primers used for qRT-PCR were designed using Primer3Plus tool (80). Primers for the reference genes *sdha* and *b-actin* were designed using Primer Express software (version 2.0.0). Oligonucleotide sequences are shown in detail in Supplementary Material, Table S1.

Eye measurements

WT and morphant embryos at 5 dpf were euthanized and fixed in 4% paraformaldehyde at 4°C overnight. Photographs were made at a fixed magnification of the dorsal view of the whole embryo with a camera (Olympus DP72) attached to a dissecting microscope (Olympus SZX 16). The cellSense imaging software (Olympus) was used to measure eye, head and body length for each embryo. Eye length was defined as the longest dimension of the elliptical eye, head length was determined from the most anterior part of the head to the otic vesicles, as previously described (81) and body length was measured from the tip of the head to the end of the trunk. The ratio of the eye size to body length (E:B) was measured to determine the relative size of the eye (40). The ratio of the eye size to head length (E:H) was measured to evaluate the effect of *six6b* depletion on eye size, independently of the head length.

For the assessment of the rescue experiments, three eye measurements from the dorsal view of embryos at 3 pdf were made. First, the eye length (defined previously) and called anterior–posterior length (AP), second the superior–inferior (SI) length defined as the longest dimension along the superior–inferior axis and third the total eye area. All measurements were traced using the Count & Measure function of the cellSense imaging software.

Histological analysis

Histological analysis was performed using standard protocols. Briefly, embryos were fixed in 4% paraformaldehyde at 4°C overnight, embedded in paraffin using standard procedures and cut in 6 μm sections. Subsequently, histological hematoxylin–eosin staining of the sections was carried out using a standard protocol.

Immunohistochemistry

Briefly, deparaffinnized sections were pretreated for antigen retrieval by microwave heating in 0.1 m sodium citrate buffer (ph 6) for time series of 9-3-3 min. Expression pattern of six6 in larvae at 3 dpf was evaluated using a rabbit polyclonal antibody against six6 (1:400, Sigma). Proliferating cells were labeled using a mouse monoclonal antibody to PCNA (1:32000,

Sigma). All antibody incubations were carried out overnight at 4°C followed by incubation with a secondary antibody (BrightVision Poly-HRP-anti-rabbit IgG or poly-HRP-Anti-mouse, respectively) and indirect immunoperoxidase labeling and hematoxylin counter stain was performed.

SUPPLEMENTARY MATERIAL

Supplementary Material is available at *HMG* online.

ACKNOWLEDGEMENTS

For the RS, we thank Ada Hooghart, Corina Brussee, Riet Bernaerts-Biskop and Patricia van Hilten for the ophthalmic data collection; Pascal Arp, Mila Jhamai, Marijn Verkerk, for their help in creating the GWAS database; Carolina Medina-Gomez and Fernando Rivadeneira for their support in creation of 1000 genomes imputed data. The authors are grateful to the study participants, the staff from the RS and the participating general practitioners and pharmacists. For the ERF study, we are grateful to all participants and their relatives, to general practitioners and neurologists for their contributions, to P. Veraart for her help in genealogy, to Jeannette Vergeer for the supervision of the laboratory work, to P. Snijders for his help in data collection and to Elisa van Leeuwen, Maarten Kooijman and Lennart Karssen for their support in creation of 1000 genomes imputed data.

Conflict of Interest statement. None declared.

FUNDING

This study was supported by Stichting Lijf en Leven. The ERF study was supported by grants from the Netherlands Organization for Scientific Research (NWO) and a joint grant from NWO and the Russian Foundation for Basic research (Pionier, 047.016.009, 047.017.043), Erasmus Medical Center, and the Centre for Medical Systems Biology (CMSB; National Genomics Initiative). Exome sequencing analysis in ERF was supported by the ZonMw grant (91111025). The generation and management of GWAS genotype data for the RS is supported by the Netherlands Organization for Scientific Research NWO Investments (nr. 175.010.2005.011, 911-03-012). This study is funded by the Research Institute for Diseases in the Elderly (014-93-015; RIDE2); the Netherlands Genomics Initiative Netherlands Organization for Scientific Research (NWO) (project nr. 050-060-810); CHANCES (nr 242244). The RS is funded by Erasmus Medical Center and Erasmus University, Rotterdam, Netherlands Organization for the Health Research and Development (ZonMw), the Research Institute for Diseases in the Elderly (RIDE), the Ministry of Education, Culture and Science, the Ministry for Health, Welfare and Sports, the European Commission (DG XII), and the Municipality of Rotterdam; M.D. Fonds; Stichting Oogfonds Nederland; Henkes Stichting; Stichting Nederlands Oogheelkundig Onderzoek; Swart van Essen; Bevordering van Volkskracht; Blindenhulp; Landelijke Stichting voor Blinden en Slechtzienden; Rotterdamse Vereniging voor Blindenbelangen; OOG; Algemene Nederlandse Vereniging ter Voorkoming van Blindheid; the Rotterdam Eye Hospital Research Foundation; Medical Workshop; Heidelberg Engineering; Topcon Europe BV.

REFERENCES

1. Kwon, Y.H., Fingert, J.H., Kuehn, M.H. and Alward, W.L. (2009) Primary open-angle glaucoma. *N. Engl. J. Med.*, **360**, 1113–1124.
2. Ramdas, W.D., Amin, N., van Koolwijk, L.M., Janssens, A.C., Demirkan, A., de Jong, P.T., Aulchenko, Y.S., Wolfs, R.C., Hofman, A., Rivadeneira, F. *et al.* (2011) Genetic architecture of open angle glaucoma and related determinants. *J. Med. Genet.*, **48**, 190–196.
3. Ramdas, W.D., Wolfs, R.C., Hofman, A., de Jong, P.T., Vingerling, J.R. and Jansonius, N.M. (2011) Lifestyle and risk of developing open-angle glaucoma: the Rotterdam study. *Arch. Ophthalmol.*, **129**, 767–772.
4. Ramdas, W.D., Wolfs, R.C., Hofman, A., de Jong, P.T., Vingerling, J.R. and Jansonius, N.M. (2011) Ocular perfusion pressure and the incidence of glaucoma: real effect or artifact? The Rotterdam Study. *Invest. Ophthalmol. Vis. Sci.*, **52**, 6875–6881.
5. Wolfs, R.C., Klaver, C.C., Ramrattan, R.S., van Duijn, C.M., Hofman, A. and de Jong, P.T. (1998) Genetic risk of primary open-angle glaucoma. Population-based familial aggregation study. *Arch. Ophthalmol.*, **116**, 1640–1645.
6. Schwartz, J.T., Reuling, F.H. and Feinleib, M. (1975) Size of the physiologic cup of the optic nerve head. hereditary and environmental factors. *Arch. Ophthalmol.*, **93**, 776–778.
7. Freeman, E.E., Roy-Gagnon, M.H., Descovich, D., Masse, H. and Lesk, M.R. (2013) The heritability of glaucoma-related traits corneal hysteresis, central corneal thickness, intraocular pressure, and choroidal blood flow pulsatility. *PLoS One*, **8**, e55573.
8. Klein, B.E., Klein, R. and Lee, K.E. (2004) Heritability of risk factors for primary open-angle glaucoma: the Beaver Dam Eye Study. *Invest. Ophthalmol. Vis. Sci.*, **45**, 59–62.
9. van Koolwijk, L.M., Despriet, D.D., van Duijn, C.M., Pardo Cortes, L.M., Vingerling, J.R., Aulchenko, Y.S., Oostra, B.A., Klaver, C.C. and Lemij, H.G. (2007) Genetic contributions to glaucoma: heritability of intraocular pressure, retinal nerve fiber layer thickness, and optic disc morphology. *Invest. Ophthalmol. Vis. Sci.*, **48**, 3669–3676.
10. Stone, E.M., Fingert, J.H., Alward, W.L., Nguyen, T.D., Polansky, J.R., Sunden, S.L., Nishimura, D., Clark, A.F., Nystuen, A., Nichols, B.E. *et al.* (1997) Identification of a gene that causes primary open angle glaucoma. *Science*, **275**, 668–670.
11. Rezaie, T., Child, A., Hitchings, R., Brice, G., Miller, L., Coca-Prados, M., Heon, E., Krupin, T., Ritch, R., Kreutzer, D. *et al.* (2002) Adult-onset primary open-angle glaucoma caused by mutations in optineurin. *Science*, **295**, 1077–1079.
12. Monemi, S., Spaeth, G., DaSilva, A., Popinchalk, S., Ilitchev, E., Liebmann, J., Ritch, R., Heon, E., Crick, R.P., Child, A. *et al.* (2005) Identification of a novel adult-onset primary open-angle glaucoma (POAG) gene on 5q22.1. *Hum. Mol. Genet.*, **14**, 725–733.
13. Wiggs, J.L., Kang, J.H., Yaspan, B.L., Mirel, D.B., Laurie, C., Crenshaw, A., Brodeur, W., Gogarten, S., Olson, L.M., Abdrabou, W. *et al.* (2011) Common variants near CAV1 and CAV2 are associated with primary open-angle glaucoma in Caucasians from the USA. *Hum. Mol. Genet.*, **20**, 4707–4713.
14. Thorleifsson, G., Walters, G.B., Hewitt, A.W., Masson, G., Helgason, A., DeWan, A., Sigurdsson, A., Jonasdottir, A., Gudjonsson, S.A., Magnusson, K.P. *et al.* (2010) Common variants near CAV1 and CAV2 are associated with primary open-angle glaucoma. *Nat. Genet.*, **42**, 906–909.
15. Burdon, K.P., Macgregor, S., Hewitt, A.W., Sharma, S., Chidlow, G., Mills, R.A., Danoy, P., Casson, R., Viswanathan, A.C., Liu, J.Z. *et al.* (2011) Genome-wide association study identifies susceptibility loci for open angle glaucoma at TMCO1 and CDKN2B-AS1. *Nat. Genet.*, **43**, 574–578.
16. Ramdas, W.D., van Koolwijk, L.M., Ikram, M.K., Jansonius, N.M., de Jong, P.T., Bergen, A.A., Isaacs, A., Amin, N., Aulchenko, Y.S., Wolfs, R.C. *et al.* (2010) A genome-wide association study of optic disc parameters. *PLoS Genet.*, **6**, e1000978.
17. Ramdas, W.D., van Koolwijk, L.M., Lemij, H.G., Pasutto, F., Cree, A.J., Thorleifsson, G., Janssen, S.F., Jacoline, T.B., Amin, N., Rivadeneira, F. *et al.* (2011) Common genetic variants associated with open-angle glaucoma. *Hum. Mol. Genet.*, **20**, 2464–2471.

18. Brown, N.L., Patel, S., Brzezinski, J. and Glaser, T. (2001) Math5 is required for retinal ganglion cell and optic nerve formation. *Development*, **128**, 2497–2508.
19. Mao, C.A., Cho, J.H., Wang, J., Gao, Z., Pan, P., Tsai, W.W., Frishman, L.J. and Klein, W.H. (2013) Reprogramming amacrine and photoreceptor progenitors into retinal ganglion cells by replacing Neurod1 with Atoh7. *Development*, **140**, 541–551.
20. Prasov, L., Nagy, M., Rudolph, D.D. and Glaser, T. (2012) Math5 (Atoh7) gene dosage limits retinal ganglion cell genesis. *Neuroreport*, **23**, 631–634.
21. Jean, D., Bernier, G. and Gruss, P. (1999) Six6 (Optx2) is a novel murine Six3-related homeobox gene that demarcates the presumptive pituitary/hypothalamic axis and the ventral optic stalk. *Mech. Dev.*, **84**, 31–40.
22. Gallardo, M.E., Lopez-Rios, J., Fernaud-Espinosa, I., Granadino, B., Sanz, R., Ramos, C., Ayuso, C., Seller, M.J., Brunner, H.G., Bovolenta, P. *et al.* (1999) Genomic cloning and characterization of the human homeobox gene SIX6 reveals a cluster of SIX genes in chromosome 14 and associates SIX6 hemizygosity with bilateral anophthalmia and pituitary anomalies. *Genomics*, **61**, 82–91.
23. Boucher, C.A., Carey, N., Edwards, Y.H., Siciliano, M.J. and Johnson, K.J. (1996) Cloning of the human SIX1 gene and its assignment to chromosome 14. *Genomics*, **33**, 140–142.
24. Ridgeway, A.G. and Skerjanc, I.S. (2001) Pax3 is essential for skeletal myogenesis and the expression of Six1 and Eya2. *J. Biol. Chem.*, **276**, 19033–19039.
25. Serikaku, M.A. and O'Tousa, J.E. (1994) Sine oculis is a homeobox gene required for *Drosophila* visual system development. *Genetics*, **138**, 1137–1150.
26. Oliver, G., Mailhos, A., Wehr, R., Copeland, N.G., Jenkins, N.A. and Gruss, P. (1995) Six3, a murine homologue of the sine oculis gene, demarcates the most anterior border of the developing neural plate and is expressed during eye development. *Development*, **121**, 4045–4055.
27. Fan, B.J., Wang, D.Y., Pasquale, L.R., Haines, J.L. and Wiggs, J.L. (2011) Genetic variants associated with optic nerve vertical cup-to-disc ratio are risk factors for primary open angle glaucoma in a US Caucasian population. *Invest. Ophthalmol. Vis. Sci.*, **52**, 1788–1792.
28. Cao, D., Jiao, X., Liu, X., Hennis, A., Leske, M.C., Nemesure, B. and Hejtmancik, J.F. (2012) CDKN2B polymorphism is associated with primary open-angle glaucoma (POAG) in the Afro-Caribbean population of Barbados, West Indies. *PLoS One*, **7**, e39278.
29. Pasquale, L.R., Loomis, S.J., Kang, J.H., Yaspan, B.L., Abdrabou, W., Budenz, D.L., Chen, T.C., Delbono, E., Friedman, D.S., Gaasterland, D. *et al.* (2013) CDKN2B-AS1 genotype-glaucoma feature correlations in primary open-angle glaucoma patients from the United States. *Am. J. Ophthalmol.*, **155**, 342–353 e345.
30. Osman, W., Low, S.K., Takahashi, A., Kubo, M. and Nakamura, Y. (2012) A genome-wide association study in the Japanese population confirms 9p21 and 14q23 as susceptibility loci for primary open angle glaucoma. *Hum. Mol. Genet.*, **21**, 2836–2842.
31. Burdon, K.P., Crawford, A., Casson, R.J., Hewitt, A.W., Landers, J., Danoy, P., Mackey, D.A., Mitchell, P., Healey, P.R. and Craig, J.E. (2012) Glaucoma risk alleles at CDKN2B-AS1 are associated with lower intraocular pressure, normal-tension glaucoma, and advanced glaucoma. *Ophthalmology*, **119**, 1539–1545.
32. Nakano, M., Ikeda, Y., Tokuda, Y., Fuwa, M., Omi, N., Ueno, M., Imai, K., Adachi, H., Kageyama, M., Mori, K. *et al.* (2012) Common variants in CDKN2B-AS1 associated with optic-nerve vulnerability of glaucoma identified by genome-wide association studies in Japanese. *PLoS One*, **7**, e33389.
33. Wiggs, J.L., Yaspan, B.L., Hauser, M.A., Kang, J.H., Allingham, R.R., Olson, L.M., Abdrabou, W., Fan, B.J., Wang, D.Y., Brodeur, W. *et al.* (2012) Common variants at 9p21 and 8q22 are associated with increased susceptibility to optic nerve degeneration in glaucoma. *PLoS Genet.*, **8**, e1002654.
34. Krimpenfort, P., Ijpenberg, A., Song, J.Y., van der Valk, M., Nawijn, M., Zevenhoven, J. and Berns, A. (2007) p15Ink4b is a critical tumour suppressor in the absence of p16Ink4a. *Nature*, **448**, 943–946.
35. Li, X., Perissi, V., Liu, F., Rose, D.W. and Rosenfeld, M.G. (2002) Tissue-specific regulation of retinal and pituitary precursor cell proliferation. *Science*, **297**, 1180–1183.
36. Adzhubei, I.A., Schmidt, S., Peshkin, L., Ramensky, V.E., Gerasimova, A., Bork, P., Kondrashov, A.S. and Sunyaev, S.R. (2010) A method and server for predicting damaging missense mutations. *Nat. Methods*, **7**, 248–249.
37. Cooper, G.M., Goode, D.L., Ng, S.B., Sidow, A., Bamshad, M.J., Shendure, J. and Nickerson, D.A. (2010) Single-nucleotide evolutionary constraint scores highlight disease-causing mutations. *Nat. Methods*, **7**, 250–251.
38. Consortium, G.T. (2013) The Genotype-Tissue Expression (GTEx) project. *Nat. Genet.*, **45**, 580–585.
39. Wagner, A.H., Anand, V.N., Wang, W.H., Chatterton, J.E., Sun, D., Shepard, A.R., Jacobson, N., Pang, I.H., Deluca, A.P., Casavant, T.L. *et al.* (2013) Exon-level expression profiling of ocular tissues. *Exp. Eye Res.*, **111**, 105–111.
40. Veth, K.N., Willer, J.R., Collery, R.F., Gray, M.P., Willer, G.B., Wagner, D.S., Mullins, M.C., Udvadia, A.J., Smith, R.S., John, S.W. *et al.* (2011) Mutations in zebrafish lrp2 result in adult-onset ocular pathogenesis that models myopia and other risk factors for glaucoma. *PLoS Genet.*, **7**, e1001310.
41. Toy, J., Yang, J.M., Leppert, G.S. and Sundin, O.H. (1998) The optx2 homeobox gene is expressed in early precursors of the eye and activates retina-specific genes. *Proc. Natl. Acad. Sci. U S A.*, **95**, 10643–10648.
42. Lopez-Rios, J., Gallardo, M.E., Rodriguez de Cordoba, S. and Bovolenta, P. (1999) Six9 (Optx2), a new member of the six gene family of transcription factors, is expressed at early stages of vertebrate ocular and pituitary development. *Mech. Dev.*, **83**, 155–159.
43. Aijaz, S., Allen, J., Tregidgo, R., van Heyningen, V., Hanson, I. and Clark, B.J. (2005) Expression analysis of SIX3 and SIX6 in human tissues reveals differences in expression and a novel correlation between the expression of SIX3 and the genes encoding isocitrate dehyhrogenase and cadherin 18. *Genomics*, **86**, 86–99.
44. Zhou, X., Hollemann, T., Pieler, T. and Gruss, P. (2000) Cloning and expression of xSix3, the Xenopus homologue of murine Six3. *Mech. Dev.*, **91**, 327–330.
45. Lagutin, O., Zhu, C.C., Furuta, Y., Rowitch, D.H., McMahon, A.P. and Oliver, G. (2001) Six3 promotes the formation of ectopic optic vesicle-like structures in mouse embryos. *Dev. Dyn.*, **221**, 342–349.
46. Carl, M., Loosli, F. and Wittbrodt, J. (2002) Six3 inactivation reveals its essential role for the formation and patterning of the vertebrate eye. *Development*, **129**, 4057–4063.
47. Amato, M.A., Arnault, E. and Perron, M. (2004) Retinal stem cells in vertebrates: parallels and divergences. *Int. J. Dev. Biol.*, **48**, 993–1001.
48. Raymond, P.A., Barthel, L.K., Bernardos, R.L. and Perkowski, J.J. (2006) Molecular characterization of retinal stem cells and their niches in adult zebrafish. *BMC Dev. Biol.*, **6**, 36.
49. Kassen, S.C., Thummel, R., Burket, C.T., Campochiaro, L.A., Harding, M.J. and Hyde, D.R. (2008) The Tg(ccnb1:EGFP) transgenic zebrafish line labels proliferating cells during retinal development and regeneration. *Mol. Vis.*, **14**, 951–963.
50. Gallardo, M.E., Rodriguez De Cordoba, S., Schneider, A.S., Dwyer, M.A., Ayuso, C. and Bovolenta, P. (2004) Analysis of the developmental SIX6 homeobox gene in patients with anophthalmia/microphthalmia. *Am. J. Med. Genet. A*, **129A**, 92–94.
51. Aijaz, S., Clark, B.J., Williamson, K., van Heyningen, V., Morrison, D., Fitzpatrick, D., Collin, R., Ragge, N., Christoforou, A., Brown, A. *et al.* (2004) Absence of SIX6 mutations in microphthalmia, anophthalmia, and coloboma. *Invest. Ophthalmol. Vis. Sci.*, **45**, 3871–3876.
52. Zuber, M.E., Perron, M., Philpott, A., Bang, A. and Harris, W.A. (1999) Giant eyes in Xenopus laevis by overexpression of XOptx2. *Cell*, **98**, 341–352.
53. Lieschke, G.J. and Currie, P.D. (2007) Animal models of human disease: zebrafish swim into view. *Nat. Rev. Genet.*, **8**, 353–367.
54. Guo, S. (2004) Linking genes to brain, behavior and neurological diseases: what can we learn from zebrafish? *Genes Brain Behav.*, **3**, 63–74.
55. Malicki, J., Neuhauss, S.C., Schier, A.F., Solnica-Krezel, L., Stemple, D.L., Stainier, D.Y., Abdelilah, S., Zwartkruis, F., Rangini, Z. and Driever, W. (1996) Mutations affecting development of the zebrafish retina. *Development*, **123**, 263–273.
56. Neuhauss, S.C. (2003) Behavioral genetic approaches to visual system development and function in zebrafish. *J. Neurobiol.*, **54**, 148–160.
57. Haffter, P., Granato, M., Brand, M., Mullins, M.C., Hammerschmidt, M., Kane, D.A., Odenthal, J., van Eeden, F.J., Jiang, Y.J., Heisenberg, C.P. *et al.* (1996) The identification of genes with unique and essential functions in the development of the zebrafish, Danio rerio. *Development*, **123**, 1–36.
58. Cheyette, B.N., Green, P.J., Martin, K., Garren, H., Hartenstein, V. and Zipursky, S.L. (1994) The Drosophila sine oculis locus encodes a homeodomain-containing protein required for the development of the entire visual system. *Neuron*, **12**, 977–996.

59. Kobayashi, M., Toyama, R., Takeda, H., Dawid, I.B. and Kawakami, K. (1998) Overexpression of the forebrain-specific homeobox gene six3 induces rostral forebrain enlargement in zebrafish. *Development*, **125**, 2973–2982.
60. Loosli, F., Winkler, S. and Wittbrodt, J. (1999) Six3 overexpression initiates the formation of ectopic retina. *Genes Dev.*, **13**, 649–654.
61. Bernier, G., Panitz, F., Zhou, X., Hollemann, T., Gruss, P. and Pieler, T. (2000) Expanded retina territory by midbrain transformation upon overexpression of Six6 (Optx2) in Xenopus embryos. *Mech. Dev.*, **93**, 59–69.
62. Del Bene, F., Tessmar-Raible, K. and Wittbrodt, J. (2004) Direct interaction of geminin and Six3 in eye development. *Nature*, **427**, 745–749.
63. Lopez-Rios, J., Tessmar, K., Loosli, F., Wittbrodt, J. and Bovolenta, P. (2003) Six3 and Six6 activity is modulated by members of the groucho family. *Development*, **130**, 185–195.
64. Dimasi, D.P., Burdon, K.P., Hewitt, A.W., Fitzgerald, J., Wang, J.J., Healey, P.R., Mitchell, P., Mackey, D.A. and Craig, J.E. (2012) Genetic investigation into the endophenotypic status of central corneal thickness and optic disc parameters in relation to open-angle glaucoma. *Am. J. Ophthalmol.*, **154**, 833–842 e832.
65. Hannon, G.J. and Beach, D. (1994) p15INK4B is a potential effector of TGF-beta-induced cell cycle arrest. *Nature*, **371**, 257–261.
66. Gonzalez-Nunez, V., Nocco, V. and Budd, A. (2010) Characterization of drCol 15a1b: a novel component of the stem cell niche in the zebrafish retina. *Stem Cells*, **28**, 1399–1411.
67. Agathocleous, M. and Harris, W.A. (2009) From progenitors to differentiated cells in the vertebrate retina. *Annu. Rev. Cell Dev. Biol.*, **25**, 45–69.
68. Hofman, A., van Duijn, C.M., Franco, O.H., Ikram, M.A., Janssen, H.L., Klaver, C.C., Kuipers, E.J., Nijsten, T.E., Stricker, B.H., Tiemeier, H. *et al.* (2011) The Rotterdam Study: 2012 objectives and design update. *Eur. J. Epidemiol.*, **26**, 657–686.
69. Aulchenko, Y.S., Heutink, P., Mackay, I., Bertoli-Avella, A.M., Pullen, J., Vaessen, N., Rademaker, T.A., Sandkuijl, L.A., Cardon, L., Oostra, B. *et al.* (2004) Linkage disequilibrium in young genetically isolated Dutch population. *Eur. J. Hum. Genet.*, **12**, 527–534.
70. Pardo, L.M., MacKay, I., Oostra, B., van Duijn, C.M. and Aulchenko, Y.S. (2005) The effect of genetic drift in a young genetically isolated population. *Ann. Hum. Genet.*, **69**, 288–295.
71. Rolando, M., Iester, M., Campagna, P., Borgia, L., Traverso, C. and Calabria, G. (1994) Measurement variability in digital analysis of optic discs. *Doc. Ophthalmol.*, **85**, 211–222.
72. Dielemans, I., Vingerling, J.R., Wolfs, R.C., Hofman, A., Grobbee, D.E. and de Jong, P.T. (1994) The prevalence of primary open-angle glaucoma in a population-based study in The Netherlands. The Rotterdam Study. *Ophthalmology*, **101**, 1851–1855.
73. Czudowska, M.A., Ramdas, W.D., Wolfs, R.C., Hofman, A., De Jong, P.T., Vingerling, J.R. and Jansonius, N.M. (2010) Incidence of glaucomatous visual field loss: a ten-year follow-up from the Rotterdam Study. *Ophthalmology*, **117**, 1705–1712.
74. Li, H. and Durbin, R. (2009) Fast and accurate short read alignment with Burrows–Wheeler transform. *Bioinformatics*, **25**, 1754–1760.
75. Brouwer, R.W., van den Hout, M.C., Grosveld, F.G. and van Ijcken, W.F. (2012) NARWHAL, a primary analysis pipeline for NGS data. *Bioinformatics*, **28**, 284–285.
76. McKenna, A., Hanna, M., Banks, E., Sivachenko, A., Cibulskis, K., Kernytsky, A., Garimella, K., Altshuler, D., Gabriel, S., Daly, M. *et al.* (2010) The Genome Analysis Toolkit: a MapReduce framework for analyzing next-generation DNA sequencing data. *Genome Res.*, **20**, 1297–1303.
77. Kimmel, C.B., Ballard, W.W., Kimmel, S.R., Ullmann, B. and Schilling, T.F. (1995) Stages of embryonic development of the zebrafish. *Dev. Dyn.*, **203**, 253–310.
78. Vilella, A.J., Severin, J., Ureta-Vidal, A., Heng, L., Durbin, R. and Birney, E. (2009) EnsemblCompara GeneTrees: complete, duplication-aware phylogenetic trees in vertebrates. *Genome Res.*, **19**, 327–335.
79. Robu, M.E., Larson, J.D., Nasevicius, A., Beiraghi, S., Brenner, C., Farber, S.A. and Ekker, S.C. (2007) p53 activation by knockdown technologies. *PLoS Genet.*, **3**, e78.
80. Untergasser, A., Nijveen, H., Rao, X., Bisseling, T., Geurts, R. and Leunissen, J.A. (2007) Primer3Plus, an enhanced web interface to Primer3. *Nucleic Acid Res.*, **35**, W71–W74.
81. van de Water, S., van de Wetering, M., Joore, J., Esseling, J., Bink, R., Clevers, H. and Zivkovic, D. (2001) Ectopic Wnt signal determines the eyeless phenotype of zebrafish masterblind mutant. *Development*, **128**, 3877–3888.